International Conference on Space Optics—ICSO 2012

Ajaccio, Corse

9–12 October 2012

Near- infrared imager and slitless spectrograph (NIRISS): a new instrument on James Webb Space Telescope (JWST)

Michael Maszkiewicz

Near- Infrared Imager and Slitless Spectrograph (NIRISS): a new instrument on James Webb Space Telescope (JWST)

Michael Maszkiewicz

Canadian Space Agency
Saint-Hubert, Qc, Canada
michael.maszkiewicz@asc-csa.gc.ca

Abstract - **The James Webb Space Telescope (JWST) is a 6.5 m diameter deployable telescope that will orbit the L2 Earth–Sun point beginning in 2018. NASA is leading the development of the JWST mission with their partners, the European Space Agency and the Canadian Space Agency.**
 The Canadian contribution to the mission is the Fine Guidance Sensor (FGS). Originally, the FGS incorporated a flexible narrow spectral band science imaging capability in the form of the Tunable Filter Imaging Module –TFI, based on a scanning Fabry–Perot etalon [1]. In the course of building and testing of the TFI flight model, numerous technical issues arose with unforeseeable length of required mitigation effort. In addition to that, emerging new science priorities caused that in summer of 2011 a decision was taken to replace TFI with a new instrument called Near Infrared Imager and Slitless Spectrograph (NIRISS). NIRISS preserves most of the TFI opto-mechanical design: focusing mirror, collimator and camera TMA telescopes, dual filter and pupil wheel and detectors but, instead of a tunable etalon, uses set of filters and grisms for wavelength selection and dispersion. The FGS-Guider and NIRISS have completed their instrument-level cryogenic testing and were delivered to NASA Goddard in late July 2012 for incorporation into the Integrated Science Instrument Module (ISIM).

 Index Terms—**James Webb Space Telescope, astronomical instrumentation, slitless spectroscopy, grism**

I. INTRODUCTION

A. Technical Issues

The optical assembly of the FGS consists of two modules: the Guider and until mid 2011 the Tunable Filter Imager (TFI). The TFI module allowed narrow–band imaging with spectral resolution R=100 in one of two wavelengths ranges: 1.6 to 2.5 µm and 3.2 to 4.9 µm [2]. The motivation for the TFI replacement with NIRISS came from the numerous technical and scientific factors concerning TIF's Fabry-Perot etalon. Many of the technical challenges encountered were successfully resolved but the remaining few proved to be very

difficult to overcome within the project schedule. At the end of the TFI development, the main identified obstacles were:

- Insufficient voltage range required for etalon gap/wedge tuning at 30K by the piezoelectric actuators (PZT).
- PZTs length variation due to hysteresis and cooling down to 30K effects.
- Uncertainty about the etalon alignment survivability during on-orbit shock events caused by the observatory mirror deployments.

In retrospective, the root causes of the etalon development failure can be summarized as:

- Lack of early truly representative prototype testing.
- Insufficient margins in the mechanical and electrical design.
- Use of the commercial PZTs [3].

B. New Science Goals

The original scientific objectives of the TFI were explanatory observation and first light detection. The latter capability was diminished already in the past when the TFI short wave channel, starting at about 1 µm, was eliminated due to the observatory mass constraints. Still, the TFI 1.5 to 1.6 µm short wavelength range was considered to be useful. However, by 2011 the epoch of re-ionization had become better defined as z=10.6±1.2 with resulting shift of Ly-α emissions to shorter wavelengths and smaller expected range of re-ionization [4, 5]. That would diminish even more the TFI first light detecting capabilities. The NIRISS instrument will bring it back by providing four observing modes: broad-band imaging between 0.9 and 5 µm, R=150 wide-field spectroscopy between 1.0 and 2.5 µm, single-object cross-dispersed slitless spectroscopy optimized for exoplanet transit spectroscopy between 0.6 and 2.5 µm at R=700, and sparse-aperture interferometric high contrast imaging between 3.8 and 4.8 µm [6].

.

II. NIRISS OPTICAL LAYOUT AND OPTICAL COMPONENTS

The NIRISS preserves great majority of the TFI configuration [1] with the biggest change consisting of the etalon removal and addition of the new pupil and filter components into the Dual Wheel. The representation of the modified TFI turned into NIRISS is shown in Fig.1 and the new configuration of the Dual Wheel is shown in Fig.2 and Fig.3. As before, the FGS Guider is located on the other side of the Optical Bench.
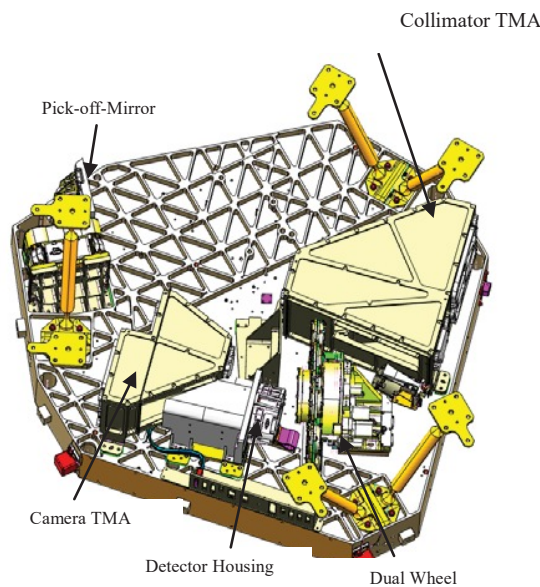

Fig.1. NIRISS Optical Bench configuration. Some baffles removed.
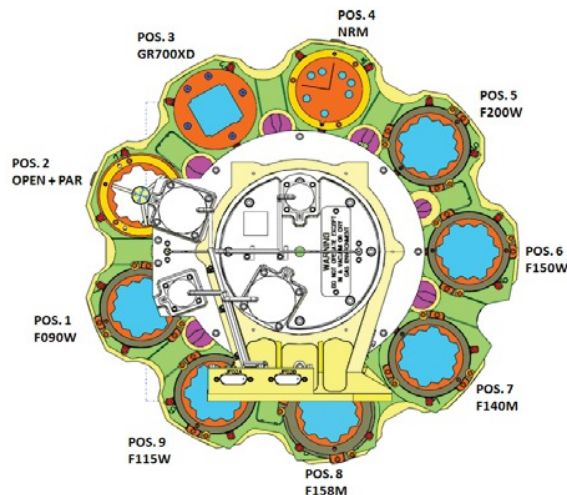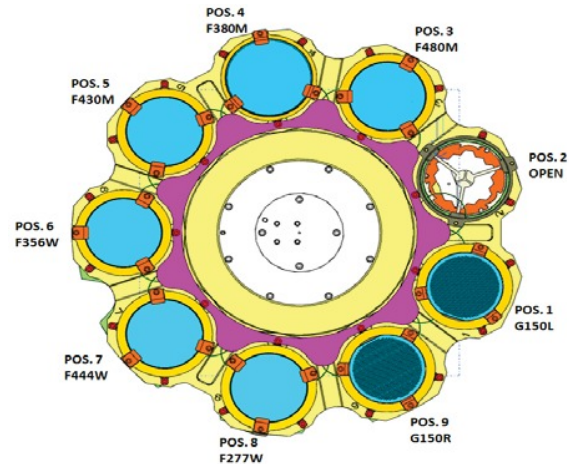

Fig.2 NIRISS pupil wheel components

Fig.3. NIRISS filter wheel components

Table I summarizes NIRISS filter, grism and mask configurations for different modes of operation. Filter numerical designation refers to central wavelengths λ_c in tens of nanometers. For example, F090W denotes $\lambda_c = 900$ nm

TABLE I

NIRISS mode	Filters	Grism	Mask
Broad Band Imaging (BBI)	F090W, F115M, F150W, F200W, F277W, F444W F356W		
Wide-Field Slitless Spectroscopy (WSS)	F115W, F150W, F200W, F140M, F158M	GR150H or GR150V	
Single Object Slitless Spectroscopy (SOSS)	OPEN	GR700XD	
Sparse-Aperture Interferometric Imaging (SAII)	F380M, F430M, F444W		Non Redundant Mask (NMR)
Pupil Alignment (used only during on-ground testing)	OPEN		Pupil Alignment Reference (PAR)

NIRISS can also be used in guiding mode with pupil and filter in OPEN positions.

III. NIRISS PERFORMANCE INDICATORS

A. Broad Band Imaging (BBI)

As illustrated in Fig.4, due to mostly reflective optics, NIRISS sensitivity is very similar to NIRCam (another JWST instrument), allowing complementary parallel mode of operation of both instruments.
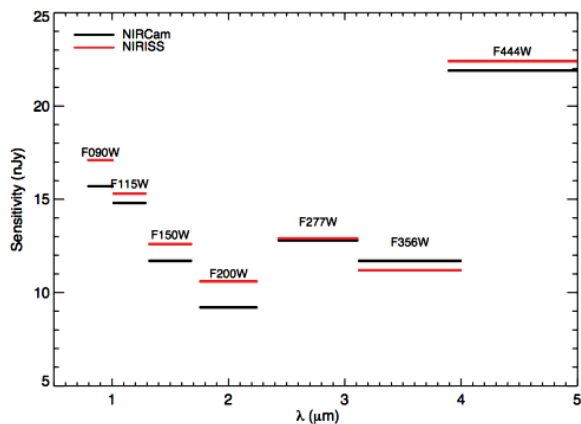
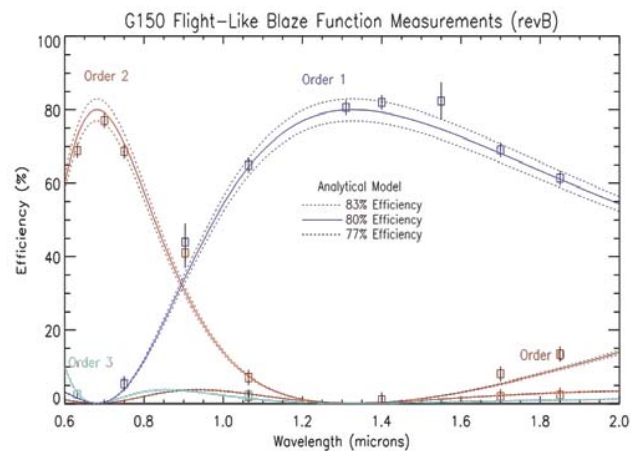Fig.4. NIRISS sensitivity in BBI mode
(10σ, 10,000s, BOL)

Fig.6. NIRISS GR150 grism efficiency curves, measured vs. modeled.

B. Wide-Field Slitless Spectroscopy (WFSS)

The WFSS mode of NIRISS operation is optimized for Lyα emitters (1-2.5 μm) and makes use of a pair of grisms GR150V and GR150H. In order to break wavelength-position degeneracy two prisms are at 90 deg angle to each other and are used in two separate imaging sessions. In this scheme, the intersection of the two perpendicular dispersion lines indicates undeviated wavelength and true sky position of the source. Both GR150 are made of infrasil 301 with resin replicated gratings. Other specifications are: resolution=150, aperture=43 mm, groove density=11.21 lines/mm, blaze angle=1.5 deg, blaze wavelength=1.3 μm and undeviated wavelength=1.05 μm. In Fig.6 GR150 blaze curve is shown as measured and compared to numerically modeled values. The modeling included groove shape imperfections deduced from the Atomic Force Microscopy (AFM) sampling.
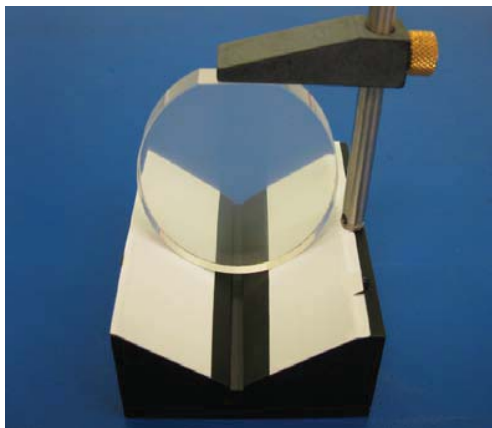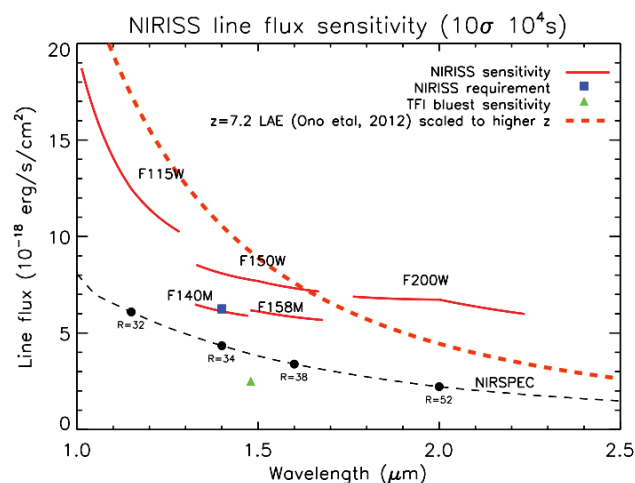

Fig.7. NIRISS sensitivity in WFSS mode.

C. Single-Object Slitless Spectroscopy (SOSS)

This mode of NIRISS operation is optimized for relatively bright stars (e.g. exoplanet transiting systems) in 0.6-2.5 μm spectral range in the first order of dispersion. It is based on a GR700XD grism made of the directly ruled ZnSe. A ZnS cross-dispersion prism is placed in front of the grism for an optimal separation of the first and second order spectra. A weak cylindrical lens, built into ZnS prism induces a defocus in spatial direction and together with 2 deg rotation about Z axis mitigates PSF spectral undersampling. Other specifications are: resolution=700, aperture=33x33mm, groove density=54.4 lines/mm, apex angle=1.9 deg, blaze angle=2.63 deg and blaze wavelength=1.25 μm. As for GR150, efficiency curves were modeled numerically to account for grooves imperfections sampled by AFM.
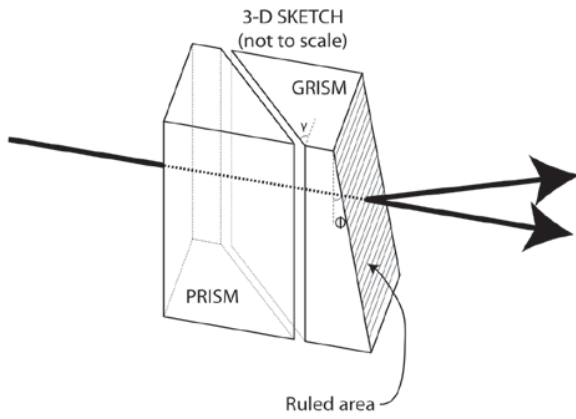

Fig.5. NIRISS GR150 grism

Fig.8. NIRISS GR700 grism -prism assembly
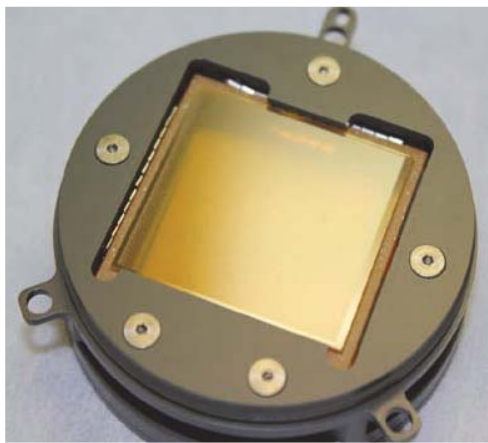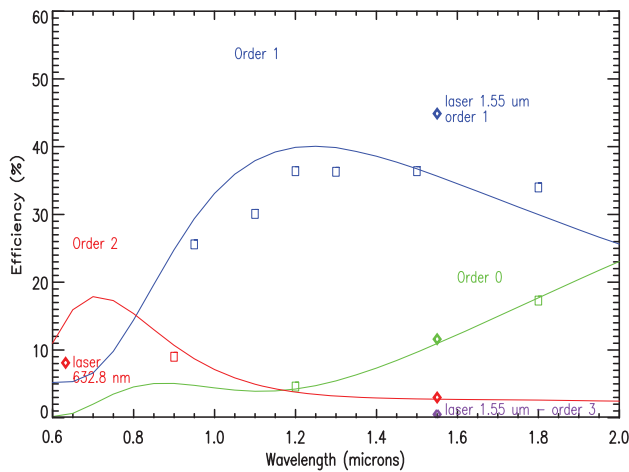

Fig.9. NIRISS GR700XD grism

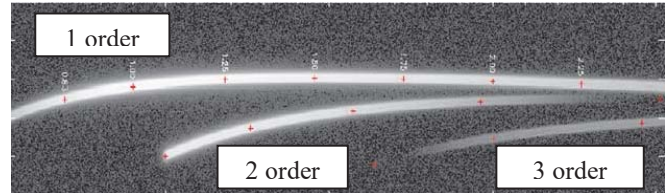Fig.10. NIRISS G700XD efficiency, measured vs. modeled

Fig. 11. NIRISS GR700XD spectra simulation

Simulation of NIRISS SOSS spectra is shown in Fig.11. The dispersion is placed along the detector fast axis and close to its edge. Reading it out via four parallel amplifiers in 256 x 2048 pixels subarray mode, will allow short integration times to increase detection dynamic range with stars brightness up to J=5.

D. Sparse-Aperture Interferometric Imaging (SAII)

The SAII is based on the use of a Non-Redundant Mask for high-contrast imaging of the exoplanets very close to their parent stars. The major change, compared to the TFI, is the removal of the coronagraphic mode (due to absence of the pupil apodization masks). The SAII spectral range extends from 3.8 to 4.8 µm covered by three medium bandwidth filters listed in Table. I. This will allow more distant (fainter) stars detection than in TFI.
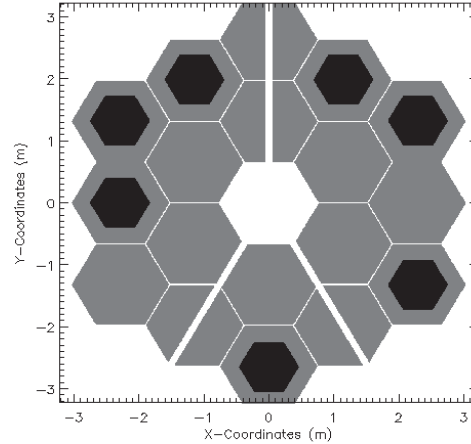

Fig.12 NIRISS NRM mask in the pupil wheel

Table II summarizes AMS performance simulation results.

TABLE II.

Star –planet separation (arcs)	0.1	0.2	0.3	0.4
Contrast (Δmag)	8.4	8.66	8.71	8.74

IV. NIRISS INTEGRATION AND TEST STATUS

The end-to-end functional and performance cryogenic vacuum testing of NIRISS was successfully completed at the beginning of 2012. The new, compared to TFI, components of the Dual Wheel went through separate qualification process afterwards. After the complete system integration, the FGS-Guider and NIRISS were transferred to NASA Goddard in July 2012 to be incorporated into the Integrated Science Instruments Module (ISIM) and for further tests.
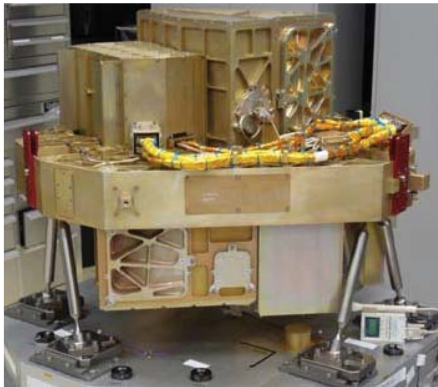

Fig.13. Fully assembled NIRISS (bottom) and FGS-Guider

REFERENCES

[1] N. Rowlands, K. Saad, J.B. Hutchings, and R. Doyon, "James Webb Space Telescope (JWST) Fine Guidance Sensor: overview'', Can. Aeronaut. Space J., Vol. 55, No.2, pp. 69-78, 2009.

[2] D. Touahri, P. Cameron, C. Evans, C. Haley, Z. Osman, A. Scott, and N. Rowlands, "Tunable Filter Imager for JWST: Etalon Opto-mechanical design and Test Results'', Proc. SPIE 7808, 78081K (2010).

[3] C. Haley, N. Roy, Z. Osman, N. Rowlands, and A. Scott, "Space environment challenges with the tunable Fabry-Pérot etalon for the JWST fine guidance sensor'', Proc. SPIE 8442, (2012)-in press.

[4] D.N. Spergel et al., "Three-year Wilkinson Microwave Anisotropy Probe (WMAP) observations: Implications for cosmology", ApJS 170, pp.377-408 (2007).

[5] E. Komatsu et al., "Seven-year Wilkinson Microwave Anisotropy Probe (WMAP) observations: Cosmological interpretation", ApJS 192, 18 (2011).

[6] R. Doyon et al., "The JWST fine guidance sensor (FGS) and near-infrared imager and slitless spectrograph (NIRISS)", Proc. SPIE 8442, (2012)-in press.